Funnel-flow accretion onto highly magnetized neutron stars and shock generation

Shigeyuki KARINO[1,2,3] , Motoki KINO[2,4] and John C. MILLER[2,5]

[1]*JAD Program, Universiti Industri Selangor, Block 4, Jln Zirkon A7/A, Seksyen 7, Shah Alam 40000, Selangor, Malaysia*
[2]*SISSA/ISAS & INFN, via Beirut 2-4, 34014 Trieste, Italy*
[3]*Shibaura Institute of Technology, Tokyo, Japan*
[4]*JAXA/ISAS, 3-1-1 Yoshinodai, Sagamihara, Japan*
[5]*Department of Physics (Astrophysics), University of Oxford, UK*

(Received Mmmmm DD, YYYY)

In this paper, we initiate a new study of steady funnel-flow accretion onto strongly magnetized neutron stars, including a full treatment of shock generation. As a first step, we adopt a simplified model considering the flow within Newtonian theory and neglecting radiative pressure and cooling. The flow is taken to start from an accretion disc and then to follow magnetic field lines, forming a transonic funnel flow onto the magnetic poles. A standing shock occurs at a certain point in the flow and beyond this material accretes subsonically onto the star with high pressure and density. We calculate the location of the standing shock and all other features of the flow within the assumptions of our model. Applications to observed X-ray pulsars are discussed.

§1. Introduction

Following the discovery of periodically variable X-ray sources[1),2)] and subsequent theoretical[4),3)] explanations, systems consisting of strongly magnetized neutron stars accreting from their binary companions have become widely accepted as providing the model for periodic X-ray sources.[5),7),6)] The accreted matter coming via Roche lobe overflow from the companion forms an accretion disc around the neutron star (NS). If the NS has a strong magnetic field ($\gtrsim 10^{12}$G), eventually at least some of the accreting matter cannot continue to accrete directly onto the NS surface in the disc plane but rather is constrained to follow the magnetic field lines, forming a funnel flow onto the magnetic poles (e.g. Ref. 4)). The polar caps reach high temperatures, emitting high-energy radiation in the form of X-rays. If the magnetic axis and the rotational axis are misaligned, this high energy radiation from the magnetic poles may be observed as periodic pulsations.[8),5),7),6)]

Polar accretion models assuming strong magnetic fields have been studied by many authors.[4),3),10),9)15),14),11),12),13)] In these studies, it has been shown that accretion onto the polar regions of strongly magnetized NSs and shock generation near to the NS surface can explain the high energy emission seen in X-ray pulsars. Almost all previous studies, however, have been limited to cylindrical or conical funnel flow aligned with the magnetic axis, whereas the actual accretion flow must have a curved geometry along the magnetic field lines going from the disc to the stellar pole. Including the effects of the curved geometry may well be very important for

understanding the complex behaviour of the light curves of X-ray pulsars.[17),16)] We here solve the flow equations in a consistent way, starting from where the funnel-flow material leaves the plane of the accretion disc and following it until it impacts on the magnetic poles.

There have been several previous studies of this type which have included the effects of the curved flow geometry.[18),21),19),13)] All of these solve the Bernoulli equation, obtaining stationary transonic flow solutions similar to Bondi accretion.[22)] In the present study, we mainly follow the approach of Koldoba et al. (2002, hereafter, KLUR).[13)] (We note that Koldoba and collaborators have subsequently carried out very interesting related calculations using an MHD computer code[34)] but these were not addressing the question of shock location which is our main interest here.) Assuming a dipole magnetic field whose axis coincides with the stellar rotation axis, KLUR constructed the equations for transonic flow and calculated accretion flows which accelerate from the subsonic regime into a supersonic regime. In their study, however, although they found the location of the transonic critical point, they did not calculate the position of the shock front. In the present work, we now extend this, following the same basic picture but calculating also the shock location and strength and the effects of shock heating. This represents the first step in a larger project to study this mechanism in full detail.

We adopt here a simplified model, considering a one-dimensional steady funnel flow along the field lines of a strictly dipole magnetic field aligned with the rotation axis, treating it within Newtonian theory and neglecting radiative pressure and cooling. Since the field is taken to be a purely dipole one (in the region of the funnel flow) we do not have any Poynting flux term in our calculation. We require the field to be strong enough to keep the funnel "rigid" and to keep the fluid flowing along the field lines: under the circumstances envisaged, this condition should be well-satisfied everywhere apart from close to where the flow leaves the disc and where it impacts on the NS surface.

We recognize that the simplifications which we are making are very significant ones but they give us a problem which can then be solved completely in a straightforward way, providing a useful basis for future work. Within the picture which we are using here, we can calculate the properties of the flow all the way from where it leaves the plane of the disc up to the stellar surface, allowing us to see several aspects which have not been observed in previous studies. In particular, we have shown that the shock location is sensitively dependent on the ratio of the pressures at the points where the flow leaves the disc and where it impacts on the NS surface. This is a crucial property of the accreting systems. Determining the shock location and the global characteristics of the flow is important for linking the properties of observed X-ray pulsars to the physical conditions in the NS – disc systems.

We want to stress that our approach here does not attempt to include any detailed treatment of the physics near to the neutron star surface or near to where the funnel flow moves out of the plane of the disc. This has been treated elsewhere by a number of authors (as described in a later section). We focus instead on how the global solution fits together, something which we consider as certainly forming a necessary framework within which to fit these other more detailed discussions of

particular parts of the flow.

The plan of this paper is as follows: in Section 2 we describe how we set up the problem. Section 3 then introduces the formulation for our treatment of transonic flow along the dipole magnetic field lines and Section 4 presents the equations for treating the standing shock. Section 5 describes our method of solution for flows including shocks and presents our results. In Section 6, several related issues are discussed. Finally, Section 7 contains a summary of the paper together with some further discussion of the results and their astronomical implications. Throughout the paper, we use standard spherical coordinates (r, θ, φ) as well as cylindrical coordinates (R, φ, z), which are convenient for some of the descriptions. The subscripts "NS" and "d" denote, respectively, that the values of the physical parameters concerned are measured at the NS surface or at the point where the funnel flow leaves the plane of the disc.

§2. Problem set-up

We are considering here a strongly magnetized neutron star with a dipole field surrounded by an accretion disc. At some point, moving in through the disc, the accretion flow becomes significantly altered due to its interaction with the magnetic field which, in turn, is distorted away from its purely poloidal form within the disc because of interaction with the disc material (see Kluzniak & Rappaport[20] for a recent treatment). Eventually, at least some part of the accreting material starts to go along the dipole field lines onto the magnetic poles of the star. As with the previous studies, we consider here a *rigidly rotating dipole field* everywhere within the region of the funnel flow, co-rotating with the neutron star.[21),18),19),13)] For a sufficiently strong magnetic field, each element of the accreting matter will fall onto the star along a single field line passing through its initial position on the disc. The geometry of the dipole field can be described by

$$r = R_{\rm d} \sin^2 \theta, \tag{1}$$

where, $R_{\rm d}$ is the distance from the centre of the star to the point where the funnel flow leaves the plane of the disc.

The dipole field strength can be written as

$$B_{\rm p}^2 = \frac{\mu^2}{r^6} \left(4 - \frac{3r}{R_{\rm d}} \right), \tag{2}$$

where $B_{\rm p}$ is the poloidal magnetic field and μ is the dipole moment. This equation gives the magnetic field strength as a function of radial coordinate r along a field line which intersects the disc at $r = R_{\rm d}$. The location of the point at which the funnel flow leaves the disc is determined by the competition between pressure, gravity and magnetic forces and is hard to estimate precisely, particularly in view of instabilities which play a role in this. We therefore simply choose suitable values for $R_{\rm d}$ and carry out our calculations with these (see Section 5).

Following KLUR, we note that transonic solutions are only possible for $R_{\rm d}$ close to the co-rotation radius $R_{\rm corot}$ (i.e., where the disc is co-rotating with the neutron

star) and so we make the approximation of assuming that the stellar angular velocity Ω coincides with the Keplerian rotation rate at $r = R_{\rm d}$; i.e.,

$$\Omega^2 = \frac{Gm}{R_{\rm d}^3}, \tag{3}$$

where G is the gravitational constant, and m is the mass of the star.

Under these conditions, the transonic accretion flow can be solved for using the method given by KLUR (see Section 3). This flow will have a shock, at a certain point in the supersonic region, which we here assume to be adiabatic and planar. Next, we introduce the further assumption that there are *no radiative energy losses* from the inflowing material; the Bernoulli equation can then be applied everywhere along the flow-lines.

Following these preparations, we can then solve for the whole stream configuration, including an adiabatic shock, if we impose suitable boundary conditions at the point where the funnel flow leaves the plane of the disc and at the stellar surface. The main goal of the calculation is to estimate the position of the standing shock and the distribution of physical quantities in the flow.

§3. Formalism for flow without a shock

Following KLUR, we solve the energy conservation equation (Bernoulli equation) with the condition that each fluid element moves along a magnetic field line going from $r = R_{\rm d}$ on the disc to the NS surface. For the present situation, we write the Bernoulli equation (in the reference frame co-rotating with the field line) as

$$E = \frac{1}{2}v^2 + \frac{a^2}{\gamma - 1} - \frac{Gm}{r} - \frac{1}{2}\Omega^2 r^2 \sin^2\theta, \tag{4}$$

where E is the specific energy (assumed to be constant), v is the poloidal velocity along the field line, a is the sound speed and γ is the adiabatic index. The last term in this plays the role of a potential corresponding to the centrifugal force. Since we are considering a *rigidly rotating dipole field* throughout the region of the funnel flow there is, by assumption, no toroidal field component present there. This assumption (which is a rather reasonable one for most of the funnel flow) allows us to omit the Poynting flux term which would otherwise appear in Eq. (4). The role of the magnetic field then consists only in fixing the configuration of the flux tube, in keeping the fluid elements moving on it and in determining the variation with position of ρv via the MHD mass conservation equation

$$4\pi\rho\frac{v}{B_{\rm p}} = K, \tag{5}$$

(where K is a constant).[24] By using Eqs. (2) and (5), the kinetic energy of the fluid related to motion along the field line can be rewritten as $v^2/2 = K^2 B_{\rm p}^2/32\pi^2\rho^2$ and inserting this into the Bernoulli equation gives

$$E = \varepsilon(r,\rho) = \frac{K^2\mu^2}{32\pi^2\rho^2 r^6}\left(4 - \frac{3r}{R_d}\right) + \frac{s\rho^{\gamma-1}}{\gamma - 1}$$

$$-\frac{Gm}{r}-\frac{1}{2}\Omega^2 r^2\sin^2\theta. \tag{6}$$

Here we have used the specific entropy, $s\equiv a^2/\rho^{\gamma-1}$ instead of the sound speed. With the assumption that the specific energy E and the specific entropy s are conserved along the flow-line, this equation gives a relationship between ρ and r and so we can calculate the density distribution $\rho(r)$ along the flow-line if we specify boundary conditions at the point of departure from the disc: $E=E(R_{\rm d})=$ const. and $s=s(R_{\rm d})=$ const.

For convenience of calculation, we rewrite Eq. (6) in the dimensionless form:

$$\tilde{E}=\tilde{\varepsilon}(\tilde{r},\tilde{\rho})=\frac{4-3\tilde{r}}{2\tilde{\rho}^2\tilde{r}^6}+\frac{\tilde{s}\tilde{\rho}^{\gamma-1}}{\gamma-1}-\left(\frac{1}{\tilde{r}}+\frac{\tilde{r}^3}{2}\right). \tag{7}$$

Here, we have used following transformation of variables,

$$\begin{aligned} &r=R_{\rm d}\tilde{r},\quad \rho=\frac{K\mu}{4\pi\Omega R_{\rm d}^4}\tilde{\rho},\\ &s=\Omega^2R_{\rm d}^2\left(\frac{4\pi\Omega R_{\rm d}^4}{K\mu}\right)^{\gamma-1}\tilde{s},\quad E=\Omega^2R_{\rm d}^2\tilde{E}. \end{aligned} \tag{8}$$

(From here on, since we use only dimensionless quantities, we will omit the tildes.) By solving Eq. (7), we can obtain the values of the physical quantities everywhere along a flow-line if there is no shock. Note that when working in terms of the dimensionless quantities, the field strength does not itself enter the calculation, only its variation with position.

We are interested in transonic solutions with the initially subsonic inflow becoming supersonic at a critical point. In order that the flow should be non-singular at the critical point (as required for a physically meaningful steady-flow solution) regularity conditions must be satisfied there, as given by Eqs. (16) and (17) of KLUR.

§4. The treatment of shocks

We will denote the location of the critical point by $r_{\rm c}$; a shock may then appear beyond this in the supersonic part of the flow with the location depending on the boundary conditions. We next summarize our methodology for treating the shock within our simplifying assumptions of considering a stationary planar shock which is adiabatic (i.e. no energy is lost from the flow).[25] From the conservation of the mass, momentum and energy fluxes across the shock, one obtains the Rankine-Hugoniot relations linking the values of quantities on either side of it. The ones of relevance for us here are:

$$\rho_2=\frac{(\gamma+1)M_1^2}{(\gamma-1)M_1^2+2}\rho_1 \tag{9}$$

$$p_2=\frac{2\gamma M_1^2-(\gamma-1)}{\gamma+1}p_1 \tag{10}$$

where $M = v/a$ is the Mach number and the subscripts 1 and 2 denote the values of flow quantities immediately before and after the shock. The shock raises the specific entropy of the fluid, with the change being given by

$$\Delta s = s_2 - s_1 = \gamma \left(\frac{p_2}{\rho_2^\gamma} - \frac{p_1}{\rho_1^\gamma} \right). \tag{11}$$

In the next section, we use these shock relations together with the flow equation (7).

§5. Accretion flow with a shock

5.1. *Flow beyond the shock*

The behaviour of the fluid quantities along the flow-line, for given boundary conditions at $r = R_{\rm d}$, is completely described by the Bernoulli equation (7) except that, when passing across the shock front, the value of the specific entropy needs to be changed to the new higher value, i.e. beyond the shock, the Bernoulli equation becomes:

$$E = \varepsilon(r, \rho) = \frac{4 - 3r}{2\rho^2 r^6} + \frac{s_2 \rho^{\gamma - 1}}{\gamma - 1} - \left(\frac{1}{r} + \frac{r^3}{2} \right), \tag{12}$$

where s_2 is the specific entropy of the flow beyond the shock, given by Eq. (11).

Our procedure for calculating the entire flow solution with the shock, starting from conditions at $r = R_{\rm d}$ on the disc and ending at the surface of the NS, is as follows: (i) Choose a position for the shock $r = r_{\rm s}$, with $r_{\rm NS} \le r_{\rm s} \le r_{\rm c}$. (ii) Solve for the flow in the region upstream of the shock, $r_{\rm s} \le r \le R_{\rm d}$, using Eq. (7). This gives the value of $\rho_1 = \rho(r_{\rm s})$, just before the shock, from which can be calculated the corresponding values of p_1 and M_1. (iii) Using the Rankine-Hugoniot relations, we then calculate the values of density and pressure beyond the shock (ρ_2 and p_2) and hence the new value of the specific entropy s_2. (iv) Using this value of s_2, we then calculate the flow beyond the shock using Eq. (12). In this procedure we obtain the value of ρ at the stellar surface and hence also the values of the other fluid parameters there. (v) In practice, we would prefer to specify the value of the pressure at the stellar surface rather than the location of the shock and so we iterate the solution until the shock location corresponding to the desired surface pressure is found.

In Fig. 1, we show our solutions for density and velocity in the special case of transonic flow with *no* shock. We have made calculations for $\gamma = 4/3$ with parameter values of $s = 0.003$ and $E = -1.448$. Note that $\gamma = 4/3$ is smaller than the maximum value of γ for which transonic flow can occur in Bondi accretion ($\gamma = 5/3$). This figure also shows the increased entropy s_2 which would appear beyond shocks occurring at different locations $r_{\rm s}$ along the flow-lines. The value of s_2 is one of the most important quantities here, since it controls the whole flow solution in the downstream region, $r_{\rm NS} \le r \le r_{\rm s}$.

Figs. 2 and 3 show the variation of density and pressure along the flow-lines; the lowest solid curve corresponds to transonic flow without a shock, as shown in Fig. 1, and the upper curves are for flows having an adiabatic shock at different locations. When there is a shock, density and temperature have discontinuous jumps across it,

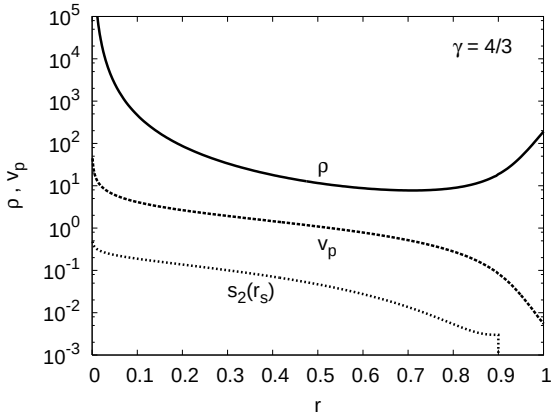

Fig. 1. Density and poloidal velocity distributions along flow-lines with no shock for different values of γ. We show the case with $\gamma = 4/3$. Behaviour of the the enhanced entropy which would appear beyond shocks occurring at different locations r_s is also shown.

as given by Eqs. (9) and (10). The envelope of the density values on the downstream side of the shock, ρ_2, is shown by the dotted curve in Fig. 2, and the envelope for p_2 is shown in the same way in Fig. 3. The behaviour of the physical quantities for $r_{NS} \leq r \leq r_s$ is given by Eq. (12). Note that the density can increase across the shock by at most a factor of $(\gamma+1)/(\gamma-1)$, within the non-relativistic theory being used here, whereas increases of several orders of magnitude may occur by means of progressive compression in the subsonic flow beyond the shock.

From Figs. 2 and 3, we see that the resulting density and pressure at the stellar surface depend sensitively on the location of the shock (as an example, $r_{NS} = 0.005 R_d$ is shown as the vertical dotted line in the figures). As mentioned previously, if the pressure (or density) at the stellar surface is given as a boundary condition, the shock location can then be determined and the whole solution completed. Note that in Figs. 2 and 3, the curves for the higher values of r_s rise quickly just beyond the shock and then flatten to an almost constant slope, whereas those for smaller r_s have an almost constant slope throughout the region beyond the shock. The reason for this difference can be understood from Eq. (12): in calculating the behaviour of the density and pressure just beyond the shock, the gravity term $\propto r^{-1}$ completely dominates over the centrifugal term $\propto r^3$ when the shock occurs near to the stellar surface, whereas the centrifugal term makes a significant contribution with respect to the gravity term further from the star. This difference is reflected in the two-component gradients of the curves in Fig. 4, introduced below.

5.2. *Pressures and densities achievable at the NS surface*

Before going into details about the shock location, we here discuss the range of possible densities in the flow at the point where it impacts on the NS surface. The *maximum* achievable density corresponds to the shock occurring just after the flow passes the critical point. In this case, the fluid reaches the NS surface with almost zero poloidal velocity and so the kinetic energy term in Eq. (12) can be neglected

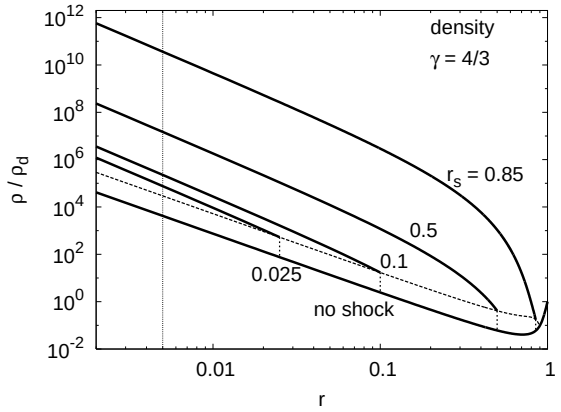

Fig. 2. Density distributions for flows including shocks, taking $\gamma = 4/3$ and $s = 0.003$. The upper solid curves are for flows with shock discontinuities at $r = 0.85, 0.5, 0.1$ and 0.025 (with the dashed lines marking the shock discontinuities); the dotted curve is the envelope of the density values on the downstream side of the shock; the lowest thick solid curve is for a flow with no shock. The vertical thin-dotted line denotes the position of the NS surface in the case of $r_{\rm NS}/R_{\rm d} = 5.0 \times 10^{-3}$.

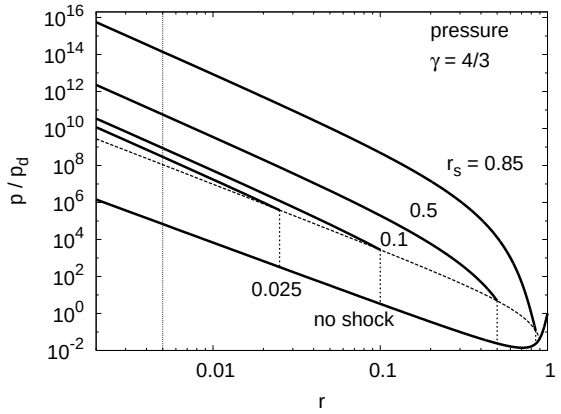

Fig. 3. Pressure distributions corresponding to the density distributions in Fig. 2.

there*). The rotational kinetic energy term at the NS surface can also be neglected since the field lines are taken to be co-rotating with the neutron star which is itself

*) This can be easily understood if we consider the analogy with Bondi accretion. Bondi flow has two trans-sonic sequences, one representing flow which is being *accelerated* from sub-sonic to super-sonic and the other representing flow being *decelerated* from super-sonic to sub-sonic. An accretion-flow solution starts off along the first (accelerated) sequence but, after the critical point, a shock may occur in which case the solution jumps down to the second (decelerated) sequence, where it is then sub-sonic. Following this, the flow is progressively decelerated. If the shock occurs very close to the critical point, there is a relatively long deceleration time before the flow reaches the stellar surface and so the velocity there will be quite low.

slowly-rotating for all of the cases of interest here. We then obtain

$$\rho_{\rm NS,max} \approx \left[\frac{\gamma-1}{s_2}\left(E+\frac{R_{\rm d}}{r_{\rm NS}}\right)\right]^{1/(\gamma-1)}. \tag{13}$$

The *minimum* achievable density corresponds to the shock occurring just above the stellar surface. In this case, the kinetic energy dominates over the thermal energy just before the shock and we obtain

$$\rho_{\rm NS,min} \approx \frac{(\gamma+1)M_{\rm 1,NS}^2}{(\gamma-1)M_{\rm 1,NS}^2+2} \times \left[\frac{R_{\rm d}^5(4R_{\rm d}-3r_{\rm NS})}{2r_{\rm NS}^5(Er_{\rm NS}+R_{\rm d})}\right]^{1/2}. \tag{14}$$

The first term on the right hand side is the factor appearing in Eq. (9).

For given outer boundary conditions $(E, s_1, R_{\rm d})$, the density in the flow at the NS surface must lie within the range between these maximum and minimum values for any flow including a shock. The range of possible pressures in the flow at the NS surface can be obtained in the same way.

5.3. *Location of the shock*

Figs. 2 and 3 show values for the normalized density and pressure along the flow-lines, plotted against the normalized radial coordinate for various shock locations. We take a canonical value of 10 km for the neutron star radius but this then corresponds to different values of $\tilde{r}$ depending on the value taken for $R_{\rm d}$, the location at which the funnel flow leaves the disc. (For our calculations, we use the following representative values for the other neutron star parameters: $m = 1.4M_\odot$, $\mu = 10^{30}$G cm^{-3} giving $B_{\rm p,NS} \approx 2.0\times10^{12}$G - see, for example, Shapiro and Teukolsky 1983).[8)]

At the outer and inner boundaries of the funnel flow we impose pressure-matching boundary conditions. When we know the starting point of the flow ($R_{\rm d}$) and the ratio of the pressures at the inner and outer boundaries ($p_{\rm NS}/p_{\rm d}$), we can obtain the appropriate shock position. Fig. 4 shows the shock position $r_{\rm s}$, normalized by the NS radius $r_{\rm NS}$, plotted against the pressure ratio $p_{\rm NS}/p_{\rm d}$ for a range of selected values of $R_{\rm d}$ ($r_{\rm NS}/R_{\rm d} = 0.1, 0.05, 0.02, 0.01, 0.005, 0.002$ and 0.001, as marked next to the related curves), taking account of the fact that the actual values of $R_{\rm d}$ are rather uncertain. The shock positions (in a log scale) are distributed within a band roughly proportional to $\log(p_{\rm NS}/p_{\rm d})$: as the pressure ratio becomes larger, the shock moves further away from the NS surface. The shock positions obtained using the various specific boundary conditions discussed below are indicated by the filled circles in this figure. We now turn to discussion of these conditions.

5.3.1. Outer boundary condition

At the outer boundary $r = R_{\rm d}$, we set the pressure in the funnel flow equal to the gas pressure at that point in the disc. We discuss here a number of possible models for this although all of them should be considered as being very approximate.

First, we consider the picture where the outer boundary of the funnel flow is matched onto a Shakura-Sunyaev disc[28)] with the funnel flow being taken to start

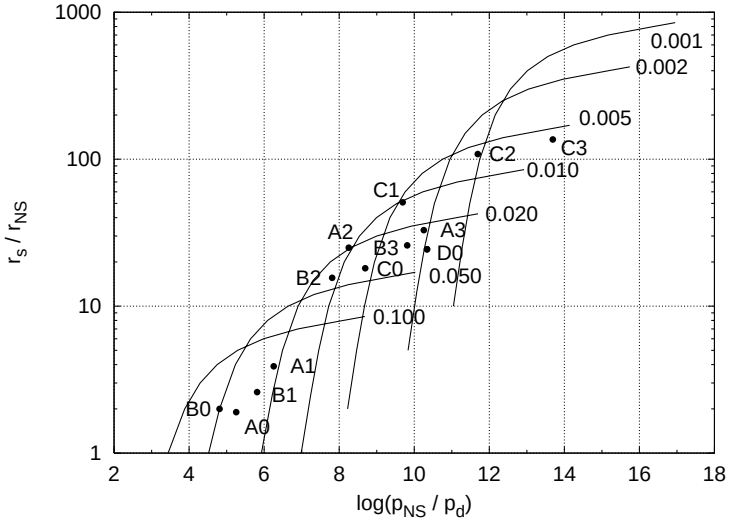

Fig. 4. Shock locations as functions of the pressure ratio. The filled circles correspond to the cases listed in Table I as indicated by the adjacent labels. The trend for the shock moving further out as the pressure ratio increases was to be expected since the stopping power of the back pressure becomes greater as the pressure ratio increases, causing it to be felt further out. The reason for the change in slope seen within each individual curve has been discussed in Section 5.1.

from the point where the magnetic pressure of the dipole field balances the gas pressure.[4] This gives

$$p_{\rm d} = \frac{B_{\rm p}(R_{\rm d})^2}{8\pi} = 4.65 \times 10^{15} \alpha^{-9/10} \times \left(\frac{R_{\rm d}}{10^7 {\rm cm}}\right)^{-51/20} \left(1 - 0.35\sqrt{\frac{10^7 {\rm cm}}{R_{\rm d}}}\right)^{4/5} . \quad (15)$$

where α is the alpha viscosity parameter (here we restrict attention to the situation for $\alpha = 0.1$). Using $B_{\rm p}(R_{\rm d})^2/8\pi = \mu^2/8\pi R_{\rm d}^6$ and fixing $\dot{m}_{\rm crit}$, this gives the value of $R_{\rm d}$ ($\dot{m}_{\rm crit}$ is the critical accretion rate which gives the Eddington luminosity). We consider models with two values of $\dot{m}/\dot{m}_{\rm crit}$: "Model A" with $\dot{m}/\dot{m}_{\rm crit} = 2/3$ and "Model B" with $\dot{m}/\dot{m}_{\rm crit} = 1$.

Our third model ("Model C") is based on the disc model of Kluzniak & Rappaport[20] who derived a modified form of the Shakura-Sunyaev solution for discs around magnetized stars, taking account of the way in which the magnetic field modifies the flow in the inner regions of the disc and is, in turn, modified by its interaction with the flow. They used two forms of ansatz for the toroidal component of the field produced in the disc (we follow their first prescription here), and calculated the effect on the flow of the resulting magnetic torque which progressively substitutes the standard viscous torque as one moves in through the disc. This gives a set of formulae for the disc profile and the variations of the fluid parameters through the disc which represent generalisations of the corresponding Shakura-Sunyaev formulae.

The standard Keplerian disc then ends at the torque balance point $r = R_{\rm torq}$ (where the magnetic torque has grown to balance the accretion torque), i.e. where

$$-R_{\rm torq}^2 B_{\rm p,torq} B_{\varphi,\rm torq} = \dot{m} \left[\frac{d(R^2\Omega)}{dR}\right]_{\rm torq}. \tag{16}$$

For the parameter values mentioned above, this comes very close to the co-rotation radius $R_{\rm corot}$ if the stellar rotation period is at the lower end of the range for X-ray pulsars. We again take the funnel flow to leave the plane of the disc at the point of balance between the gas pressure and the magnetic pressure of the dipole field; this balance occurs very close to the torque balance point. Our Model C has a Kluzniak-Rappaport disc with the same overall parameters as Model A above and has an NS rotation period of 1 second for which $R_{\rm torq}$ is indeed very close to $R_{\rm corot}$ (and $R_{\rm d} \sim R_{\rm corot}$ as required for our overall picture).

Finally, we consider the situation when the outer accretion flow consists of matter coming essentially in free-fall from a companion star and the funnel flow starts at the Alfvén radius $r_{\rm A}$ given by

$$\frac{B_{\rm p}^2}{8\pi} = \frac{1}{2}\rho(r_{\rm A})v^2(r_{\rm A}). \tag{17}$$

We then take $R_{\rm d} = r_{\rm A}$ and we refer to this case as our "Model D".

5.3.2. Inner boundary condition

At the inner boundary $r = r_{\rm NS}$, the fluid flow changes from being essentially radial to being transverse and the situation there is even less clear than at the outer boundary since we must consider a matching with the transverse pressure (including magnetic pressure) at a suitable height in the NS atmosphere. The flow pressure at the NS surface might then be as high as that given by balance with the magnetic pressure $p_{\rm NS} = B_{\rm p,NS}^2/8\pi \sim 10^{23}$dyn cm^{-2}.

Sophisticated NS atmospheric models give various different views about the NS surface pressure. For instance, Van Riper[26] found that the density of the outermost layer of the atmosphere of a magnetized NS should be in the range $\sim 0.5-10$g cm^{-3}, for $m \approx 1.0M_\odot$, $r_{\rm NS} \approx 10^6$cm, and $B_{\rm NS} \approx 10^{12}$G. However, the corresponding pressure is strongly temperature dependent and so even if we fix on $\rho \approx 1$g cm^{-3}, the pressure can take a wide range of values going from $\approx 10^{16}$dyn cm^{-2} up to $\approx 10^{22}$dyn cm^{-2} for the temperature ranging from $T \sim 10^7$K to $\sim 10^9$K. The temperature at $r = r_{\rm NS}$ is almost independent of the shock position (as discussed in Section 5.4), giving $T_{\rm NS} = 2.4 \times 10^9$K for $\alpha = 0.1$. According to Van Riper,[26] for $T_{\rm NS} \sim 10^9$K, the pressure of the NS surface layer is roughly $\sim 10^{21} - 10^{22}$dyn cm^{-2}.

On the other hand, Brown and Bildsten[29] suggested that the accreted matter cannot spread out until it reaches a greater depth, since the magnetic pressure is always much larger than the matter pressure at the polar cap. In this case, our pressure boundary condition should be modified to $\sim 10^{25}$[dyn cm^{-2}], and the height of the shock above the neutron-star surface would become much larger.

Another example of an atmosphere model for an accreting NS is the plane-parallel thin-slab model of Harding et al.[27] According to this, the density in the

atmosphere changes by about five orders of magnitude within a thin layer of width $\lesssim 200$ cm with very little accompanying change in temperature.

Detailed consideration of the physics of the near-surface region is beyond the scope of the present paper which focuses instead on global properties of the flow. Because of the uncertainties involved, we consider here a range of values for $p_{\rm NS}$, bearing in mind the atmospheric pressures quoted in above references, and we will return to give a more complete treatment of the near-surface region in future work.

From Fig. 4, it can be seen that the shock location comes closer to the NS surface when either (1) the NS surface pressure is low, or (2) the pressure is high at the point where the funnel flow leaves the disc, i.e. when the ratio $p_{\rm NS}/p_{\rm d}$ is small, the shock will occur near to the NS surface. In the opposite limit, the shock will occur far above the NS surface, similar to the situation considered by Basko and Sunyaev.[9] As discussed in Sec. 6.2 below, the steep pressure gradient occurring in an optically thick radiative accretion column would effectively lead to a rather low NS surface pressure, bringing the shock nearer to the NS surface. Results for the various specific disc models, and for a relevant range of values of $p_{\rm NS}$, are listed in Table I and depicted in Fig. 4. Cases A0, B0, C0 and D0 are the ones with the optically thick radiative columns.

Table I. Shock positions for selected surface conditions: Shakura-Sunyaev disc with moderate accretion (A), Shakura-Sunyaev disc with critical accretion (B), Kluzniak-Rappaport disc with moderate accretion (C) and the Free-fall model (D). The cases with optically thick radiative accretion columns are indicated by a $*$, and for those models, the inner boundary condition for the funnel flow is imposed at the top of the column (see Sec. 6.2).

Disc Model	NS Surface Condition $p_{\rm NS}$[dyn/cm^2]	Shock Position $r_{\rm s}$[cm]	Label
Shakura-Sunyaev disc with	1.0×10^{18} $(*)$	1.9×10^{6}	A0
$\dot{m}/\dot{m}_{\rm crit}=2/3$	1.0×10^{19}	3.9×10^{6}	A1
$R_{\rm d}=4.4\times10^{7}$ [cm]	1.0×10^{21}	25.0×10^{6}	A2
$p_{\rm d}=5.6\times10^{12}$[dyn/cm^2]	1.0×10^{23}	32.9×10^{6}	A3
Shakura-Sunyaev disc with	1.0×10^{18} $(*)$	2.0×10^{6}	B0
$\dot{m}/\dot{m}_{\rm crit}=1$	1.0×10^{19}	2.6×10^{6}	B1
$R_{\rm d}=3.7\times10^{7}$ [cm]	1.0×10^{21}	15.6×10^{6}	B2
$p_{\rm d}=1.5\times10^{13}$[dyn/cm^2]	1.0×10^{23}	25.9×10^{6}	B3
Kluzniak-Rappaport disc	1.0×10^{18} $(*)$	18.1×10^{6}	C0
$\dot{m}/\dot{m}_{\rm crit}=2/3$	1.0×10^{19}	50.9×10^{6}	C1
$R_{\rm d}=1.6\times10^{8}$ [cm]	1.0×10^{21}	108.4×10^{6}	C2
$p_{\rm d}=2.0\times10^{9}$[dyn/cm^2]	1.0×10^{23}	136.3×10^{6}	C3
Free-fall model	1.0×10^{18} $(*)$	22.4×10^{6}	D0
$R_{\rm d}=3.1\times10^{8}$ [cm]			
$p_{\rm d}=4.6\times10^{7}$[dyn/cm^2]			

§6. Discussion of related issues

6.1. *Departure of the funnel flow from the plane of the disc*

In discussing the disc models above, we estimated the location of the point where the funnel flow leaves the plane of the disc by assuming that the magnetic pressure of the dipole field of the NS balances the pressure of the accreting gas there, following Pringle & Rees.[4] This seems a reasonable approximation but there are a number of issues that make the situation less clear. First, we should stress that there is a distinction to be made between the place where material starts to leave the plane of the disc and the place where one should define the "inner edge" of the disc to be, although they are often treated as being the same. In an accreting system, the "inner edge" is not a completely clear concept although one can take it to be the place where the disc ceases to be nearly Keplerian in the case of a geometrically thin disc. Also, while one often takes the disc to be "thin", nevertheless it does have a vertical structure and conditions are certainly not constant through the height of it. It is likely that there will be a separation between some material which goes into the funnel flow while other material continues in or near the disc plane. Another point is that the pressure-balance argument is based on supposing that the poloidal field of the neutron star is not affected by its interaction with the disc material whereas, in fact, there will be at least some region where the material flow distorts the field lines producing a toroidal component within the disc and giving a torque on the accreting material, as mentioned earlier. Finally, there is the issue of a variety of instability mechanisms which can influence the situation. It is therefore clear that the question of how and where material leaves the disc plane to go into the funnel flow is a complicated one.

Following the pioneering study by Ghosh and Lamb,[11] many authors have worked to improve understanding of the magneto-hydrodynamic properties of accretion discs but this still remains a difficult subject. Frequently, the position of the "inner edge" of the disc is taken to come at the point of balance between the magnetic torque and the accretion torque (see the discussion in Section 5.3.1) with the flow remaining essentially Keplerian down to that point. This is the case for the Kluzniak-Rappaport model which we have used[20] and there one finds that the pressure balance point is extremely close to the torque balance point for parameter values of interest here. However, this depends on the ansatz made there for describing the toroidal field B_φ and, while that seems a rather reasonable one, this is something which should, in the end, come from a calculation including all of the physical features concerned. In basic MHD treatments of discs, the effective inner radius is almost coincident with the co-rotation radius, $R_{\rm corot}$,[32),31)] but some more detailed studies suggest that it may be significantly inward of this, at $R_{\rm torq} \sim 0.1 R_{\rm corot}$.[19] Alternatively, its location may be related to the Alfvén radius, as in Model D in our treatment.[33]

Even if the gas pressure does balance the magnetic pressure at the starting point of the flow, the magnetic pressure would then grow very rapidly along the flowlines (as $\sim r^{-6}$) and would soon become dominant so as to establish the funnel-

like geometry of the flow. This would then be expected to persist until the gas pressure could catch up with the magnetic pressure again after the flow penetrates into the NS surface layers.

6.2. *Radiative effects*

In the above treatment, we have not included the effects of radiation emitted by the fluid comprising the funnel flow but, in realistic situations, radiation pressure and radiative energy losses will be important near to the stellar surface. We will include these effects consistently in our future work but here we make just a rough estimate of how radiation pressure would change the present results. For doing this, we join our flow solution onto the solution for an accretion column calculated by Inoue,[10] which does include radiation pressure. Inoue (1975) solved the fluid equations, including photon diffusion, for a short accretion column just above the NS surface and found that the density distribution can be written as

$$\rho = \rho_{\rm NS}\left(\frac{r}{r_{\rm NS}}\right)^{-6}\exp\left[\frac{3(r_{\rm NS}-r)}{r_{\rm diff}}\right], \tag{18}$$

where, $r_{\rm diff} = \kappa_{\rm th}\dot{m}/8\pi c$ with $\kappa_{\rm th}$ being the Thomson scattering opacity. This density distribution (and the corresponding pressure distribution) has quite a strong dependence on r and the accretion column becomes optically thin rather close to the NS surface. In this solution, the pressure of the column decreases by roughly five orders of magnitude within the optically thick regime.

According to Inoue, the height of the optically thick radiative zone will be $\sim 6\times10^5$cm for $\dot{m} = 10^{17}$g s^{-1}.[10] When we join our solution at the top of the column with the density and pressure obtained from Eq. (18), the resulting shock position is closer to the stellar surface. Taking the pressure at the top of the radiative column ($\tau = 1$) to be $\sim 10^{18}$dyn/cm^2 and the outer boundary condition to be that for Shakura-Sunyaev disc model with $\dot{m} = \frac{2}{3}\dot{m}_{\rm crit} \simeq 10^{17}$g cm^{-1} (Model A), the shock position is then just above the top of the radiative column. This means that the flow becomes optically thick just after the shock and then emits high energy photons as black body radiation. If, on the other hand, we take the same pressure at the top of the radiative column but use the free-fall condition (Model D) for the inner boundary condition, the shock position is then still far from the NS surface and from the top of the radiative column ($r_{\rm s} = 22.4\times10^6$cm). Hence, in this case the flow becomes dense and achieves high temperatures beyond the shock, but it is still optically thin there and so emits energy via free-free radiation or cyclotron processes before forming the optically-thick radiative column. This optically-thin, but actively radiating region corresponds to a "transition region".[10),9)]

6.3. *Temperature distribution*

In this subsection, we present some results for the temperature distribution beyond the shock, as estimated using $T \equiv s\gamma^{-1}\rho^{\gamma-1}$. In Fig. 5, the temperature distribution for a transonic flow with no shock is shown by the lower solid curve and the corresponding temperature distributions for shocked flows with the selected values of $r_{\rm s}$ are also shown (cf Figs. 2 and 3). It is interesting that the tempera-

ture curves beyond the shock are independent of the shock position. This can be understood from the solution of the Bernoulli equation: since the kinetic energy is negligible beyond the shock, we have

$$T \propto \frac{\gamma - 1}{\gamma} \left[E + \frac{1}{r} + \frac{r^3}{2} \right]. \tag{19}$$

Since γ and E are constants, the temperature behaves as a function only of r and does not depend on the shock position.

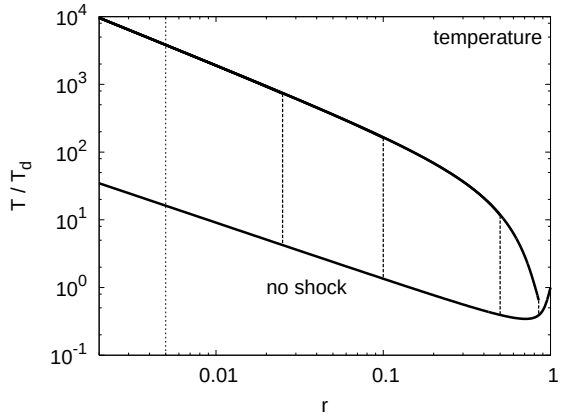

Fig. 5. Temperature distribution along the flow-lines, taking $\gamma = 4/3$.

We note that the shock is not in the highest-temperature part of the flow (although the temperatures beyond the shock are considerably higher than those before it) and that there are parts of the shocked flow at relatively lower temperatures when r_s becomes larger. Radiation from that part of the flow may appear in the low energy components of the observed spectra of X-ray pulsars. Also, if the shock heating occurs away from the stellar rotational axis, relatively hot fluid will exist in a broad region covering the stellar pole. The distribution of hot matter may change the pulse shapes: if the accretion flow emits radiation from a broad region, the geometry of the emitting flow will be changed and this may change the shape of the pulses (see, for example, Ref. 16)). As noted above, the estimates for the shock location given here are not precise but a comparison between these shock locations and the observed properties of X-ray pulsars would be interesting.

Fig. 5 shows temperatures measured in units of T_d and for converting these into actual temperature estimates, one needs to use suitable models for the disc and for the departure of the funnel flow from it. We feel that it is necessary to be cautious about interpreting these results directly in terms of actual temperatures in the flow and at the neutron star surface, both because of the diversity of the models and also because of the simplified treatment in this sub-section. However, we note that surface temperatures derived from this, for the models which we have been considering, lie in the range from $\sim 10^9$ K (standard disc case; this value is consistent with values often quoted: see, for example, Ref. 29)) to $\sim 10^{11}$ K (free-fall case; this value is too

high for actual X-ray pulsars and would indicate that energy losses from the funnel flow needed to be taken into account).

§7. Summary and further discussion

In this study, we have considered funnel-flow accretion onto a magnetized neutron star (NS), including taking into account the possible occurrence of a standing shock. We have assumed that the funnel flow goes strictly along the magnetic field lines and that the field is a dipole field, aligned with the stellar rotation axis, throughout the region of our calculation. The funnel flow leaves from the plane of the disc and accelerates smoothly into the supersonic regime, passing through a critical point. Then, at some point after this, a standing shock occurs beyond which the flow then accretes sub-sonically onto the neutron star. We have calculated the location of the standing shock, neglecting energy losses, and have obtained a full solution for given boundary conditions at the stellar surface and at the point where the funnel flow leaves the disc. The results suggest that the shock position depends strongly on the boundary conditions. As the ratio between the pressures at the inner and outer boundaries becomes larger, the shock location goes further from the NS surface. If the NS boundary pressure is high and free-fall type accretion occurs, the shock location must then be rather far above the stellar surface and the situation is as discussed by Basko and Sunyaev.[9] In contrast, the column solution given by Inoue (1975) indicates that the shock would be much closer to the NS surface.[10] As a limiting case, Braun and Yahel suggested that the shock occurs just *on* the NS surface, and in some cases cannot occur at all.[35] However, if the NS boundary pressure becomes quite high,[29] the shock front may be further out and determining its location will depend on complicated physics. A lot of studies of accretion flow onto magnetized NSs have considered flow only just near to the NS surface;[36] global treatment of the flow going from the disc to the NS has been considered by only a limited number of authors.[18),21),19),13]

The shock location may affect the spectra, luminosities and light curves of X-ray pulsars. The result that the shock location may be rather distant from the stellar surface has two implications for observations of X-ray pulsars. Firstly, as discussed in the previous section, the lower limit for the temperature of the shocked flow (at low temperatures for shocked material but much hotter than the unshocked material) depends only on the shock location. The region which has reached high temperatures due to shock heating, but is still optically thin, corresponds to the transition region discussed by Inoue and Basko & Sunyaev.[10),9] The spectrum of an X-ray pulsar will correspond to the radiation coming from the NS surface, from the optically thick radiative region, and from this transition region. The information obtained about the transition region is therefore relevant for modelling the observed properties of X-ray pulsars. Secondly, if the shock is far above the stellar surface, the radiating area presented by the shocked material will be large and the amount of radiation coming from the sides of the funnel flow will be significant. This radiation from the side-faces ("fan-beams") has a different energy range and pulse phase compared with radiation emitted in the direction along the field lines ("pencil-beams"). This

difference between the pulse phases makes the observed light curve complicated: having a large radiative region due to a distant shock location makes the fan-beam component larger, leading to irregular light curves with phase-inversion, twin-peaks, peak splitting and so on.[5),17),16)] From observed light curves and spectra, it should become possible to deduce the shock locations.

The analysis carried out in this paper has been very simplified. In actual bright X-ray sources, the complicated features which we have neglected may be important, especially near to the stellar surface. The main additional features concerned are: (i) *Radiation pressure:* the radiation energy density can become quite high near to the stellar surface and radiation pressure can dominate over gas pressure there. In Section 6.2 we have estimated the effects of this in just a rough way; we will return to give a more thorough treatment of it in future work. (ii) *Radiative energy losses:* in this paper we have neglected energy losses due to radiation emitted from the flow. However, this simplification is not valid near to the stellar surface where emissivity due to thermal bremsstrahlung becomes significant compared with the internal energy density of the flow and then, in the optically thick regime, black body radiation will become more efficient. These effects should be included in a more complete treatment. The energy losses may make the shock position move nearer to the star because they lower the pressure of the column mainly after the shock and hence the shock would occur further downstream. (iii) *Oblique dipole field:* in order for a neutron star to be an X-ray pulsar, the dipole axis must not, in fact, coincide with the rotation axis. (iv) *Relativistic effects:* neutron stars are compact objects with strong gravitational fields and also the funnel-flow velocity before the shock is quite high in some cases. Therefore both general and special relativistic effects may change the results quantitatively. (v) *Boundary conditions:* there are serious uncertainties concerning the boundary conditions both at the stellar surface and at the point where the funnel flow leaves the accretion disc. All of the above require further work but we believe that the present calculations represent a useful first step and grasp the overall nature of these accretion flows.

Acknowledgements

We thank S. Konar, N. Kawakatu, M. Takahashi, R. Takahashi and W. Kluzniak for helpful discussions.

References

1) R. Giacconi, H. Gursky, E. Kellogg, E. Schreier and H. Tananbaum, Astrophys. J. Lett. **167** (1971), L67.
2) H. Tananbaum, H. Gursky, E. M. Kellogg, R. Levinson, E. Schreier and R. Giacconi, Astropys. J. Lett. **174** (1972), L143.
3) F. K. Lamb, C. J. Pethick and D. Pines, Astrophys. J. **184** (1973), 271.
4) J. E. Pringle and M. Rees, A & A **21** (1972), 1 .
5) N. E. White, J. H. Swank and S. S. Holt, Astrophys. J. **270** (1983), 711.
6) L. Bildsten, D. Chakrabarty, J. Chiu, M. H. Finger, D. T. Koh, R. W. Nelson, T. A. Prince, B. C. Rubin, D. M. Scott, M. Stollberg, B. A. Vaughan, C. A. Wilson, and R. B. Wilson, Astrophys. J. Sapl. **113** (1997), 367.
7) F. Nagase, PASJ **41** (1989), 1.

8) S. L. Shapiro and S. Teukolsky, Black Holes, White Dwarfs and Neutron Stars, Wiley, (1983) New York.
9) M. M. Basko and R. A. Sunyaev, MNRAS **175** (1976), 395.
10) H. Inoue, PASJ **27** (1975), 311.
11) P. Ghosh and F. K. Lamb, Astrophys. J. **223** (1978), L83.
12) S. H. Langer and S. Rappaport, Astrophys. J. **257** (1982), 733.
13) A. V. Koldoba, R. V. E. Lovelace, G. V. Ustyugova and M. M. Romanova, Astron. J. **123** (2002), 2019 (KLUR).
14) A. I. Tsygan, A & A **60** (1977), 39.
15) P. Ghosh, C. J. Pethick and F. K. Lamb, Astrophys. J. **217** (1977), 578.
16) W. Nagel, Astrophys. J. **251** (1981), 278.
17) Y. M. Wang and G. L. Welter, A & A **102** (1981), 97.
18) J. Li, Astrophys. J. **456** (1996), 696.
19) J. Li and G. Wilson, Astrophys. J. **527** (1999), 910.
20) W. Kluzniak and S. Rappaport, arXiv:0709.2361 (2007).
21) G. Paatz and M. Camenzind, A & A **308** (1996), 77.
22) H. Bondi, MNRAS **112** (1952), 195.
23) R. F. Elsner, and F. K. Lamb, Astrophys. J. **215** (1977), 897.
24) R. V. E. Lovelace, C. Mehanian, C. M. Mobarry and M. E. Sulkamen, Astrophys. J. Supl. **62** (1986), 1.
25) L. D. Landau and E. M. Lifshitz, Fluid Mechanics, Pergamon Press, (1959) Oxford.
26) K. A. Van Riper, Astrophys. J. **329** (1988), 339.
27) A. K. Harding, P. Mészáros, J. G. Kirk and D. J. Galloway, Astrophys. J. **278** (1984), 369.
28) N. I. Shakura and R. A. Sunyaev, Astron. Astrophys. **24** (1973), 337.
29) E. F. Brown and L. Bildsten, Astrophys. J. **496** (1998), 915.
30) P. Ghosh and F. K. Lamb, Astrophys. J. **234** (1979), 296.
31) Y. M. Wang, Astrophys. J. **449** (1995), L153.
32) Y. M. Wang, Astron. Astrophys. **183** (1987), 257.
33) Y. M. Wang, Astrophys. J. **465** (1996), L111.
34) M. M. Romanova, G. V. Ustyugova, A. V. Koldoba and R. V. E. Lovelace, Astrophys. J. **578** (2002), 420.
35) A. Braun and R. Z. Yahel, Astrophys. J. **278** (1984), 349.
36) J. G. Kirk, Proc. ASA **5** (1984), 446.